

An Ultrasound Wearable System for the Monitoring and Acceleration of Fracture Healing in Long Bones

Vasilios C. Protopappas, *Student Member, IEEE*, Dina A. Baga, Dimitrios I. Fotiadis*, *Member, IEEE*, Aristidis C. Likas, *Senior Member, IEEE*, Athanasios A. Papachristos, and Konstantinos N. Malizos

Abstract—An ultrasound wearable system for remote monitoring and acceleration of the healing process in fractured long bones is presented. The so-called USBone system consists of a pair of ultrasound transducers, implanted into the fracture region, a wearable device and a centralized unit. The wearable device is responsible to carry out ultrasound measurements using the axial-transmission technique and initiate therapy sessions of low-intensity pulsed ultrasound. The acquired measurements and other data are wirelessly transferred from the patient-site to the centralized unit, which is located in a clinical setting. The evaluation of the system on an animal tibial osteotomy model is also presented. A dataset was constructed for monitoring purposes consisting of serial ultrasound measurements, follow-up radiographs, quantitative computed tomography-based densitometry and biomechanical data. The animal study demonstrated the ability of the system to collect ultrasound measurements in an effective and reliable fashion and participating orthopaedic surgeons accepted the system for future clinical application. Analysis of the acquired measurements showed that the pattern of evolution of the ultrasound velocity through healing bones over the postoperative period monitors a dynamic healing process. Furthermore, the ultrasound velocity of radiographically healed bones returns to 80% of the intact bone value, whereas the correlation coefficient of the velocity with the material and mechanical properties of the healing bone ranges from 0.699 to 0.814. The USBone system constitutes the first telemedicine system for the out-hospital management of patients sustained open fractures and treated with external fixation devices.

Index Terms—Fracture healing, remote patient monitoring, ultrasound, wearable devices.

I. INTRODUCTION

FRACTURE healing of long bones is a complex regenerative process that gradually restores the functional and mechanical bone properties, such as load-bearing capacity, stiff-

ness, and strength. Currently in clinical practice, assessment of fracture healing is performed by clinical and radiographic examination. Clinical examination of the affected bone is a subjective method that strongly depends on orthopaedic surgeon's experience, whereas the interpretation of plain X-rays is largely a matter of clinician's expert judgment [1]. Incorporation of quantitative information into the orthopaedists' decision-making process may assist them in detecting complications (e.g., delayed unions or nonunions) that might necessitate a prompt conservative or even surgical intervention, early assessing the endpoint of healing, and accurately determining the time-point for fixation removal.

Several methods, such as single photon absorptiometry, dual-energy X-ray absorptiometry, and quantitative computed tomography (QCT) have been used to measure the bone mineral density (BMD) of the regenerative tissue (i.e., callus) and relate it with the stiffness and strength of the healing bone [2]–[4]. On the other hand, a large corpus of work has been focused on the direct measurement of the healing bone's mechanical properties. Various techniques have been developed to determine the axial and/or bending stiffness of bones by attaching strain gauges to external fixation devices or to custom-made frames [5]–[7]. Clinical studies [5], [6] have shown that a bending stiffness of 15 Nm/degree can be used as a safe criterion for functional bony union. In other techniques, the vibrational behavior of the healing bone is studied using accelerometers and microphones [8]–[10], or the bone mechanical integrity is investigated using the acoustic emission technique [11]. The above techniques have demonstrated their potential to provide useful indications of the structural integrity of the healing bone. However, they are influenced by extrinsic bone properties, such as bone gross geometry, fracture type, etc. and also they cannot measure the properties of the callus tissue itself. Besides this, the majority of the abovementioned techniques may only take place in clinical settings requiring the intervention of a specialist to configure the measuring setup and a number of them [5], [7], [11] necessitate the temporary removal of the external fixation device.

Ultrasonic methods have extensively been employed as a monitoring tool in fracture healing. Some researchers have utilized conventional ultrasonic imaging to discriminate between the different phases of osteogenesis [12], whereas the majority of the research groups have used a transmitter-receiver configuration to measure the ultrasound propagation velocity [9], [13]–[26] and attenuation [18], [20], [21] of healing bones. In this so-called axial-transmission technique, a set of two or more ultrasound transducers (with central frequency in the

Manuscript received August 6, 2004; revised February 6, 2005. This work was supported in part by the European Union under the FP5 IST-2000-26350 USBone project (A Remotely Monitored Wearable Device for the Monitoring and Acceleration of Bone Healing). *Asterisk indicates corresponding author.*

V. C. Protopappas is with the Department of Medical Physics, Medical School, University of Ioannina and the Unit of Medical Technology and Intelligent Information Systems, Computer Science Department, University of Ioannina, GR 45110 Ioannina, Greece.

D. A. Baga is with the Unit of Medical Technology and Intelligent Information Systems, Computer Science Department, University of Ioannina, GR 45110 Ioannina, Greece.

*D. I. Fotiadis is with the Unit of Medical Technology and Intelligent Information Systems, Computer Science Department, University of Ioannina, GR 45110 Ioannina, Greece and also with the Biomedical Research Institute—Forth, GR 45110 Ioannina, Greece (e-mail: fotiadis@cs.uoi.gr).

A. C. Likas is with the Unit of Medical Technology and Intelligent Information Systems, Computer Science Department, University of Ioannina, GR 45110 Ioannina, Greece and also with the Biomedical Research Institute—Forth, GR 45110 Ioannina, Greece

A. A. Papachristos and K. N. Malizos are with the Department of Medicine, School of Health Sciences, University of Thessalia, GR 412 22 Larissa, Greece.

Digital Object Identifier 10.1109/TBME.2005.851507

range from 0.2 MHz to 2.5 MHz) are placed percutaneously (i.e., external to the skin) at a known in-between distance. The ultrasound velocity, which in general is given by the square root of the modulus of elasticity to the density of the propagating media, is determined by the transit time of the first-arriving wave that propagates along the long axis of the bone. Animal [14], [20] and clinical studies [14], [15], [17], [20] have demonstrated that the velocity of completely healed bones reaches at least 80% that of intact bones. However, the pattern of velocity evolution as healing progresses has not been quantified and no distinction has been made between partially healed bones and nonunions. Moreover, the correlation between the velocity and the mechanical properties of the healing bone has been found to range from poor [16] to moderate [14], [20] values. Major disadvantages of the percutaneous measurements are that the overlying soft tissues affect the repeatability and accuracy of the measurements and that the method is only applicable to peripheral skeletal sites, such as the tibia and radius. Simulation models [22]–[25] and experiments on immersed thin plates, bars, and bone specimens [19], [22], [24], [26] have recently been employed to investigate the nature of the propagating waves through intact and osteoporotic bones.

In addition to the diagnostic capabilities of ultrasound, low-intensity pulsed ultrasound (LiUS) has been shown in numerous *in vivo* studies to be able to accelerate the healing time by up to 38% and increase the mechanical and material properties of the healing bone [27]–[32]. LiUS is applied transcutaneously for 15 or 20 min/day by the manual attachment of a head module onto the skin above the affected region. The transmitting wave consists of 200- μ sec bursts of 0.5–1.5 MHz sine waves (depending on the application), with a pulse repetition rate of 1 KHz and average intensity of 30 mW/cm². Recently, the first transosseous (through the bone) application of LiUS on an animal osteotomy model was reported [32]. In that study, LiUS energy was transmitted through a thin stainless-steel pin that was inserted into the bone, proximal to the osteotomy site, by means of a transducer mounted on the free end of the pin. The findings of the study demonstrated that transosseous LiUS is a safe and effective alternative for accelerating fracture healing. Accelerating the time of healing is associated with major clinical, social and economical importance [33], considering that about 5%–10% of all untreated fractures will eventually fail to heal [30]. The Food and Drug Administration approved the intervention of transcutaneous LiUS for fresh fractures in 1994 and for established nonunions in 2000.

Medical wearable systems have recently been introduced into many clinical applications as a response to the need for remote monitoring and treatment of patients in home and outdoor environments [34]. Those systems typically involve the data collection unit with sensors that can be attached to the patient (e.g., patches), worn (such as a ring, shirt) or even implanted and the communication with a centralized unit based in a hospital, the doctor's office or a health provider. Wearable systems have been used for the treatment of cardiovascular diseases, the management of patients with chronic diseases [35], etc. Although current research aims to extend their application to numerous other clinical areas, many systems are yet to be fully validated and are still in the design phase. Trends in wearable technology involve

distributed sensors, context-aware devices and ubiquitous computing [36].

The purpose of this work is 1) to present an ultrasound wearable system for both remote monitoring and acceleration of the healing process in long bones and 2) to demonstrate the validation of the system on an animal study. The proposed system (USBone—Ultrasound in Bone healing) incorporates a pair of miniature ultrasound transducers, a wearable device and a centralized unit. The novelty of the USBone system consists in that the ultrasound transducers are implanted into the fracture region and the wearable platform supports the wireless communication of data from the patient's site to a centralized system. The USBone system aims to address the need for the continuous out-hospital management of patients, sustained open fractures and treated with external fixation devices, and also to provide orthopaedic surgeons with a quantitative estimation of the healing progress.

The USBone system has been applied to a sheep osteotomy model. In this paper, we focus on the description of the system's architecture, the evaluation of its functionality and the analysis of the ultrasound measurements obtained from the animal experiment. The significance of the ultrasound propagation velocity to monitor the healing progress and to correlate with the material and mechanical bone properties is demonstrated. The exploitation of the collected dataset for the construction of the system's monitoring capabilities is also discussed.

II. SYSTEM DESCRIPTION

The USBone system consists of a pair of miniature ultrasound transducers, a wearable device and a centralized unit. The transducers are implanted into the fracture region in contact with the bone surface, operating in an axial-transmission mode. The wearable device, which is a custom-made preindustrial prototype, is responsible to initiate therapy sessions of LiUS, carry out ultrasound measurements and wirelessly communicate data with the centralized unit. The centralized unit, located in a clinical environment or a health professional's premises, is an integrated patient management system and has also been designed to incorporate an automated diagnosis module to provide decision-support to health professionals. The centralized unit is accessible by orthopaedic surgeons through a web-based user interface. The system architecture is illustrated in Fig. 1.

The motivation for implementing a wearable device was the provision of a continuous and automated means for monitoring the healing status, while the patient is at home or in outdoor environments. The wireless platform is a rational design choice for the remote communication between the patient and the orthopaedic surgeon. Moreover, the centralized unit responds to the health professionals' requirement for managing many patients for a prolonged period of time.

A. Implantable Transducers

Custom-made disk-shaped unfocused contact ultrasound transducers have been used (Lead Metaniobate piezoelectric material, custom product, Valpey Fisher). The transducers generate and receive longitudinal waves at their resonant frequency (1 MHz, 70% broadband). They are encapsulated in

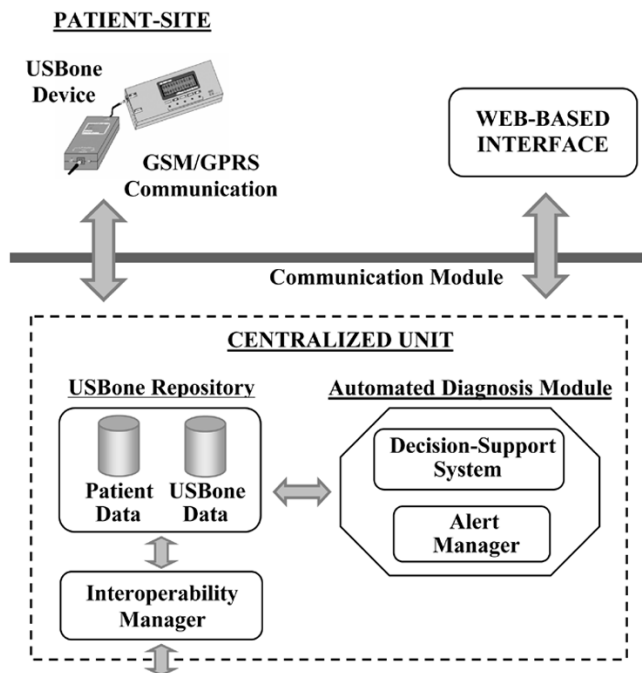


Fig. 1. The USBone system architecture. The wearable device wirelessly communicates with the centralized unit, while health professional have access to the system through a web-based interface. The centralized unit consists of the USBone repository that records both patient-related information and USBone-specific data, the interoperability manager responsible for data exchange with external CPRs, and the automated diagnosis and alert manager module that is designed to incorporate decision support to health professionals.

a specially-machined plastic case, suitable for their implantation into the fracture site and they are as small as 6 mm in thickness and 8 mm in diameter (Fig. 2). The case, made from acrylonitrile butadiene styrene, meets the biocompatibility requirements in terms of the material itself [37] and the nature of implantation that produces no wear debris. The transducers are mounted on each side of the fracture line, perpendicular to and in contact with the bone surface. The details of the implantation procedure are presented in Section III-A. For the monitoring purposes, one transducer acts as transmitter and the other as receiver, whereas for the LiUS treatment both serve as emitters of ultrasonic energy.

The motivation for the transducers' implantation is that it supports transosseous wave propagation, acquisition of signals directly from the region of interest and efficient transfer of LiUS to the fracture site. The transducers' technical specifications were selected in accordance with 1) the literature on the LiUS application [27]–[30] and 2) similar studies on ultrasonic testing of bone [18], [19], [23], [24], [26]. Their dimensions and shape were determined by the orthopaedic surgeons involved in our study.

B. USBone Wearable Device

The USBone device is a wearable and battery-operated prototype, applicable to fracture cases treated with external fixation devices. Our objective was to develop a device that is light, unobtrusive to the patient's activities and easy-to-use. In this respect, the device has been divided into two subsystems, the sensing module (SM) and the control module (CM) (Fig. 3).

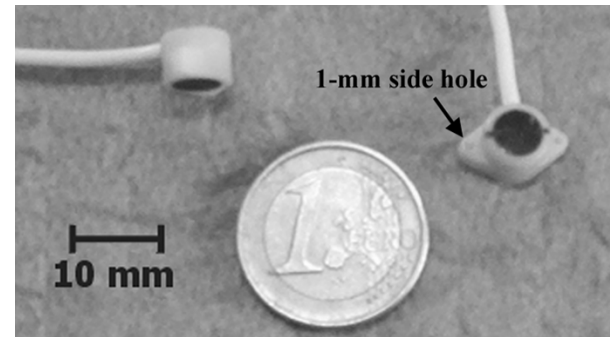


Fig. 2. The implantable ultrasound transducers, with special case design including two 1-mm side holes and silicon rubber co-axial cables.

The SM is a pulser-receiver of ultrasound (size: 78 mm × 49 mm × 25 mm, weight: 112 g) that is easily attached to the frame of the external fixator by means of a hook. The SM's role is to excite the ultrasound transmitter and acquire the received signals. The SM uses a programmable negative-going, high-voltage pulse generator (pulse width from 0.5 to 10 μ s, voltage level from -100 V to -300 V). The receiver driving stage of the SM is responsible for the acquisition, amplification (programmable gain: input full-scale sensitivity ranging from 2.5 mV to 20 mV) and digitization (sampling rate at 40 Mb/s, 10-b resolution, averaging up to 100 acquisitions) of the ultrasound signals. The SM also performs temperature readings using two thermistor-type sensors (negative temperature coefficient thermistor, measurement range 35 °C–42 °C, accuracy 0.1 °C), one attached at the affected limb and the second one at the body (reference value) to alert for possible infection (pin-track infection is not infrequent in external fixation treatment).

The CM (size: 119 mm × 49 mm × 29 mm, weight including battery: 186 g) contains the battery of the USBone wearable device (rechargeable Li-Ion battery, 3.6 V/1150 mAh) and incorporates the data storage module, a low-stage alert module, the user interface module, and the communication module. The CM can be carried on the patient's belt, which facilitates access to the device functions. The CM is interconnected to the SM for the transfer of the acquired data and for power supply purposes. Typical power consumptions are: < 25 mA at standby and < 350 mA at LiUS application (for LiUS parameters in accordance with the literature). Up to ten ultrasound signals and numerous temperature readings can be locally stored. The user interface module of the CM incorporates an alphanumeric 2 × 12 LCD display, a buzzer, and four control and one ON/OFF buttons. Moreover, the CM has the functionality of a mobile phone being able to process both global system for mobile communications (GSM) and general packet radio service (GPRS) data (embedded GSM/GPRS application). The centralized unit communicates wirelessly with the CM to long-term schedule monitoring and therapy plans (rate, duration, and intensity of LiUS, signal acquisition parameters, etc.) or order immediate action. The CM initiates LiUS sessions and ultrasound/temperature readings according to the stored schedule, while the display and the buzzer inform the patient 5 min before and throughout these procedures. The acquired measurements and other data (logs and alerts) are automatically uploaded to the centralized

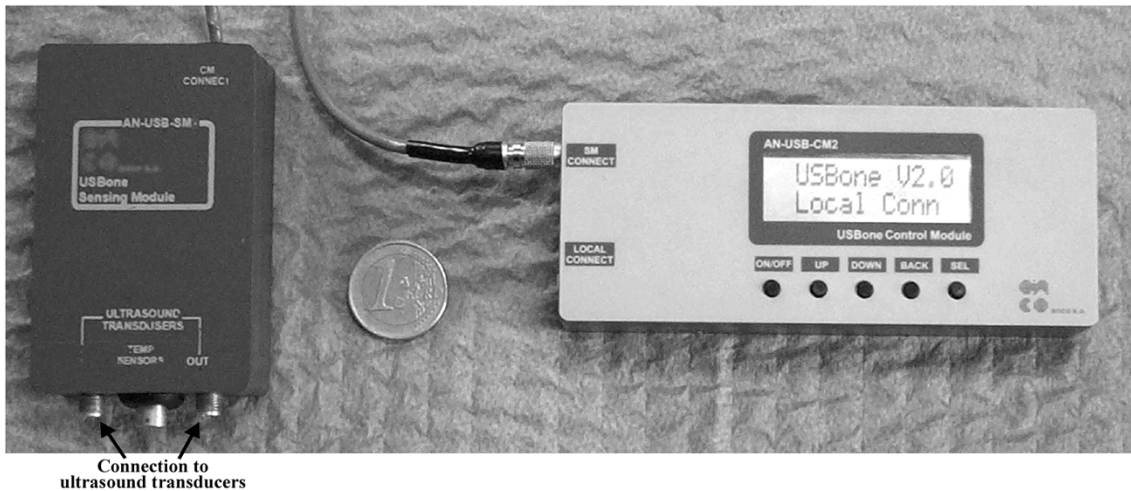


Fig. 3. The wearable USBone device. The SM (left) has two ultrasound channels and two temperature channels and is also interconnected to the CM (right). The CM incorporates one ON/OFF button, four buttons to access the mobile phone's functionality, one LCD display to inform the user of its function and one serial port for the local connection to a computer.

unit. In cases where no connection can be established, the CU stores the measurements for later transmission. In addition, the patient can also communicate with health professionals through short message service (SMS) messages. The CM can also be locally connected to a computer system (through a serial RS232 interface).

Another functionality of the device is the detection of alert situations. Alerts concern a list of predefined cases which refer to the operation of the device (low-battery and device internal faults) and to signal acquisition. A preliminary signal analysis provides indications for higher (or lower) level of signal amplification, implant deterioration or bone fragments' malalignment. Signal analysis is performed locally in the CM and is currently based on the extraction of simple waveform features, namely the starting-point and maximum amplitude of the ultrasound signal. Critical alert values are: $> 20 \mu\text{s}$ for signal arrival and $< 5 \text{ mV}$ for maximum amplitude and have been determined from lab-bench experiments on bone specimens. Local signal analysis also includes the detection of temperature difference between the affected limb and the body reference value. The critical value is $> 0.5 \text{ }^\circ\text{C}$ and has been specified by the orthopaedic surgeons. Both device and signal alerts are transmitted to the centralized unit.

Both SM and CM incorporate a reduced instructed set computer microcontroller and are implemented in full surface-mount technology on a 4-layer and 6-layer printed circuit board, respectively. Currently, five identical USBone devices have been implemented and used for the purposes of the experiment.

C. Centralized Unit (CU)

The CU is a basic patient management system and the core computational facility of the USBone system. It records patient-related data, communicates simultaneously with several USBone devices, analyzes the acquired signals, monitors patient progress, and issues alerts to orthopaedists. Health professionals can access the CU to consult patient information and remotely

schedule therapy and monitoring sessions. The CU contains four subsystems: the USBone repository, the interoperability manager, the automated diagnosis and alert manager and the user interface.

The USBone Repository is designed to incorporate both basic patient management and USBone specific information. It has been developed as a Health Level 7 (HL7—version 3.0) compatible application and, thus, enables exchange of data with other HL7-compatible computer patient records (CPRs) that may hold useful patient-related information. The recorded data form four conceptual groups; the patient identification information, the patient admission data, the medical data (including the prescribed orthopaedic treatment, X-rays, other examinations, etc.) and the USBone specific data. The USBone specific data refer to all kinds of information related to the system covering both in-hospital and out-hospital information. These data include the acquired measurements, device or system alerts, logs and device programming (i.e., rate, duration, and intensity of LiUS, acquisition parameters, etc.).

The user interface of the CU provides access to the system through a web-base interface either using a PC or a personal digital assistant.

The CU is also designed to automatically send device or system alerts to the orthopaedic surgeons in the form of an e-mail or SMS message.

The system will be integrated by constructing a diagnostic module to provide decision-support to health professionals. The dataset collected from the animal study will be exploited for the development and evaluation of the system's monitoring abilities.

III. SYSTEM VALIDATION

The USBone system has been evaluated on an animal study. The motivation for the animal model was the evaluation of the system functionality, the standardization of the transducers implantation, the investigation of the efficacy of LiUS and the construction of an ultrasound dataset for monitoring purposes.

A. Animal Fracture Model

An animal study on 40 skeletally mature sheep (42–50 Kg, 2.0–3.5 years old) was carried out. Thirty animals had the transducers implanted and were used for the monitoring purposes of the study. The remaining 10 animals were only involved in the study of the LiUS effect on the healing process which is not presented in this paper. The study received permission from the Veterinary Directorate of the Prefecture of Karditsa, Greece, according to Greek legislation and in conformance with the Council Directive of the European Union.

In the operating room, under sterilized field and general anesthesia, a transverse osteotomy was performed at the mid-shaft of the left tibia using an oscillating saw leaving a 2-mm fracture gap (Fig. 4). Reduction and stabilization of the bone fragments was performed with a unilateral, one-plane external fixation device (Stryker, Hoffmann Monotube™) using a four-pin technique. The ultrasound transducers were mounted on the bone surface, without removing the periosteum, in the anterolateral plane by means of suture (Vicril® 0, Ethicon) passing through two 1-mm diameter side-holes machined on the transducers' case. Rigid attachment was secured by looping the suture round the cortex using a blunt surgical tool and with biological respect for the surrounding soft tissue envelope. Effort was made to consistently keep the transducers' distance at 25 mm throughout all animal operations. However, their distance ranged from 20–25 mm, depending on the flatness of the cortex.

B. Experimental Protocol

For each of the 30 animals, ultrasound measurements were taken:

- from the intact tibia, before osteotomy (baseline measurement);
- immediately after the osteotomy;
- on a 10-day basis for the first postoperative month;
- on a 4-day basis until the end of the study.

Measurements were carried out using a local connection of the USBone device to a laptop computer. A number of measurements were performed remotely to evaluate the functionality of the system. Each measurement consisted of the recording of an ultrasound signal with 200 μ s duration, 10-b resolution and 40 Mb/s sampling rate. The transmitter was excited by a 200 V, 0.5 μ s negative-going pulse. The recorded signal was the average waveform of 8 successive acquisitions. Averaging was performed automatically by the ultrasound device and was used to increase the signal-to-noise ratio. The acquisition parameters were predetermined from *in vitro* experiments on cadaveric bone specimens. Temperature readings were obtained daily for the first postoperative weeks in order to assess any possible infection.

All measurements and other subject-related information were systematically recorded in the USBone Repository System. All test subjects were sacrificed on the 100.6 ± 2.9 postoperative days with intravenous injection of Pentothal. Both the healing and the contralateral (intact) tibiae were harvested. Soft tissues and the periosteum were carefully removed and the bone speci-

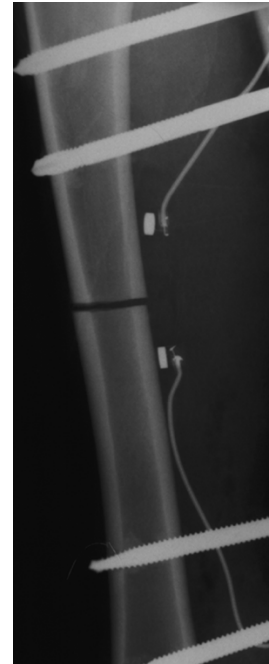


Fig. 4. An X-ray (anteroposterior view) taken immediately after the transducers' implantation. The 2-mm transverse osteotomy and the pins of the external fixation are also shown.

mens were kept frozen below -20°C stored in double airtight bags to ensure the preservation of their mechanical properties.

C. Ultrasound Signal Analysis

The ultrasound propagation velocity was determined as the ratio of the transducers' in-between distance to the time-of-flight (TOF), where TOF is the transition time of the first-arriving signal (FAS). The criterion for determining the FAS was a threshold set at 10% of the amplitude of the first signal extremum. Such a criterion minimizes erroneous estimation of the TOF as opposed to other criteria based on constant thresholds, zero-crossings, signal extrema, etc., which are affected by frequency-dependent attenuation, mode interference and other waveguidance phenomena [19], [22]–[24], [26].

D. Radiographic Assessment

Plain radiographs were taken in two planes (anteroposterior and lateral) immediately postoperatively and on a 10-day basis until the end of the study. Assessment of the radiographs was made blindly in independent reviews by two orthopaedic surgeons, according to the criterion for bony union introduced by Heckman *et al.* [28]. The cortical bridging of four cortices (two on the anteroposterior and two on the lateral radiography) was investigated and when three of four cortices were fully bridged, a fracture was considered radiographically healed. In our study, the radiographic evaluation was regarded as the Golden Standard for bony union assessment.

E. Bone Density Measurements

QCT scans were performed to measure the BMD of both the healing and contralateral bone specimens (Phillips Secura Computer Tomograph, acquisition parameters: 140 KV,

220 mA, slice thickness 2 mm, slice distance 1 mm). A solid bone phantom was used during the scanning, containing five samples with known hydroxyapatite concentrations in order to plot the Hounsfield Units-to-BMD curve. A 50-mm long region of the healing specimen, including the newly formatted callus at the level of the former osteotomy, was scanned (total of 49 slices). As for the contralateral intact specimens, a 3-mm long region was scanned at the corresponding osteotomy level (2 slices). All CT images were taken in Digital Imaging and Communications in Medicine (DICOM) format and were further processed with the use of Analyze® (Mayo Foundation, Rochester, MN).

Firstly, the average BMD value of the contralateral bones was calculated. On each QCT slice, an initial seed point was manually selected within the area of the cortical bone and a 200 mg/cm^3 threshold [2] was selected to determine the bone cortex region. The average BMD value of the region was then computed for each of the two slices to provide the average BMD value of the three-dimensional (3-D) volume of the contralateral specimen. Secondly, the average 3-D BMD of callus in the healing bones was determined using a similar approach. On each QCT slice, the region between the contours of endosteal and periosteal callus was defined using the same seeded region-growing technique and the 200 mg/cm^3 threshold. This region was further segmented into two subregions; the first is the bone cortex and the second the newly-formed callus [Fig. 5(a)]. This was performed using an empirical threshold which was set as the average BMD of the contralateral intact tibia minus two standard deviations. Finally, the average BMD of the callus segment was computed for each slice and the 3-D average callus BMD was determined [Fig. 5(b) and (c)].

F. Biomechanical Testing

Both the healing and the contralateral tibiae were biomechanically evaluated using a destructive three-point bending testing. Prior to the test, the specimens were thawed at room temperature. The specimens were positioned horizontally against two round-shaped supporters equidistant from the former fracture level with a span of 110 mm. The custom-made load head of the mechanical device (INSTRON 8871) was also rounded to minimize shear stress and cutting, and applied vertically to the bone at the fracture level with a constant speed of 20 mm/min until failure. The breaking loads were measured and the load-deflection curves were obtained. Stiffness was calculated as the linear part of the load-deflection curve, and the Young's modulus E and ultimate strength (breaking stress) σ were derived using [38]

$$E = \frac{F}{d} \cdot \frac{L^3}{48I} \quad (1)$$

$$\sigma = \frac{FLc}{4I} \quad (2)$$

where c is the distance of the load head from the center of the mass, F is the applied load, d is the deflection, L is the span length, and I is the cross-sectional moment of inertia (CSMI). Due to the complex and irregular periosteal callus shape and in order to avoid the commonly-used approximation of a circular or elliptical cross section of the bone, the position of the center

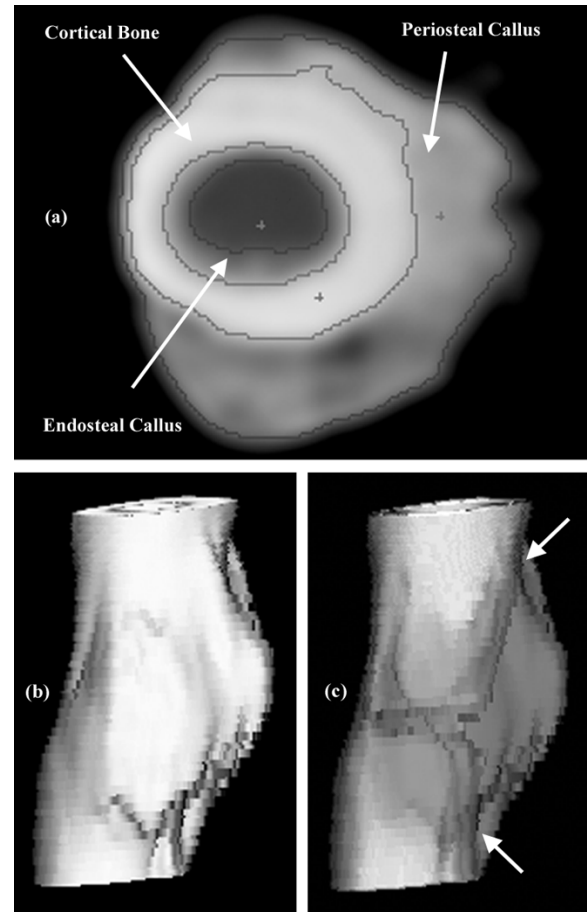


Fig. 5. (a) Segmentation of the QCT slice into the cortical bone region and the endosteal and periosteal callus regions, (b) 3-D reconstruction of the healing bone specimen (anteroposterior view), (c) pseudo-colored representation of the newly-formatted callus. Note that image enhancement has taken place in (c) for a better callus visualization. The two arrows depict the sites of the transducers' positioning.

of mass and the CSMI were computed from the corresponding QCT slices using our in-house program. Nevertheless, we assume that the neutral axis of the bending passes through the center of mass [3], [39]. In addition, because Young's modulus is practically underestimated in three-point bending testing, due to the developed shear stresses, we used the slope of the elastic region of the curve to approximate the ratio F/d [3].

G. Statistical Analysis

The inter-observer agreement on the assessment of radiographic bony union was evaluated using the McNemar's test. The Wilcoxon nonparametric test was utilized to investigate the significance of the difference in 1) the ultrasound velocity that was measured on the last postoperative day, 2) callus BMD, and 3) bone's biomechanical data, between radiographically healed and nonhealed bones. The ability of the velocity, measured on the last postoperative day, to discriminate between radiographically healed and nonhealed bones is evaluated using receiver operating characteristic (ROC) curve analysis. The Pearson correlation coefficient was used to analyze the degree of association between the ultrasound velocity, measured on the last postoperative day, and the densitometric and biomechanical measures. Statistical significance was accepted for $p < 0.05$.

IV. RESULTS

A. System Validation

The performance of the overall system components has been evaluated on the animal study in terms of system integration, functionality and usability. The receiver-stage of the SM provides undistorted signals and offers flexible data acquisition parameters (excitation pulse, amplification level, averaging number, measurement schedule, etc.) to suit various measurement conditions. The CM requires no expertise on its operation and the battery autonomy was about 8 days (typical usage: 20 min/day LiUS and one measurement-uploading daily). The wireless connectivity proved consistent and the mean uploading time was 70 s using GSM modem in indoor environment. The opinion of the orthopaedic surgeons involved in the study is that the weight of the SM does not interfere with the stability of the external fixator and the dimensions of both the modules are acceptable for clinical application. The orthopaedists found the environment of the centralized unit functional and the recorded information (both patient-related and USBone-specific) suitable for an integrated patient management system. Furthermore, the provision of web-based access to the system, the remote interaction with the device and the automated data collection make feasible the monitoring of many patients by a doctor in a very efficient way.

B. Animal Study

One animal was lost during anaesthesia and two due to pulmonary infection and thromboembolism postoperatively (not related to the application of the system). Additionally, measurements were not successfully collected for three animals due to problems associated with the animals tampering with the measuring system. Therefore, a complete ultrasound dataset was successfully constructed for 24 of the 30 animals, consisting of about 400 measurements.

No major complications occurred postoperatively. Temperature readings, recorded for the first postoperative weeks, did not show any difference between the body and the affected region temperature. No negative findings were observed from the use of implants. Radiographic examination showed no radiolucent circumference around the transducers and, during specimen harvesting, abundant fibrosis was observed without any sign of local biological reaction.

The ultrasound signal waveforms taken 1) from the intact bone, 2) immediately after osteotomy, 3) at the seventh, and 4) at the fourteenth postoperative week of an animal are depicted in Fig. 6. The propagation velocity was determined from each waveform by measuring the transition time of the FAS. We investigated the evolution of velocity over the healing time. Three typical evolution patterns were observed among all the test subjects. The first pattern [Fig. 7(a)] was observed for 19 animals, the second for 3 animals [Fig. 7(b)] and the third for 2 animals [Fig. 7(c)].

The first velocity evolution pattern [Fig. 7(a)] illustrates an initial reduction in velocity after the osteotomy has been performed, which is explained by the biological fluids that fill the 2-mm fracture gap and have lower velocity (1450 m/s). On average for all the animals in the group, the velocity just after

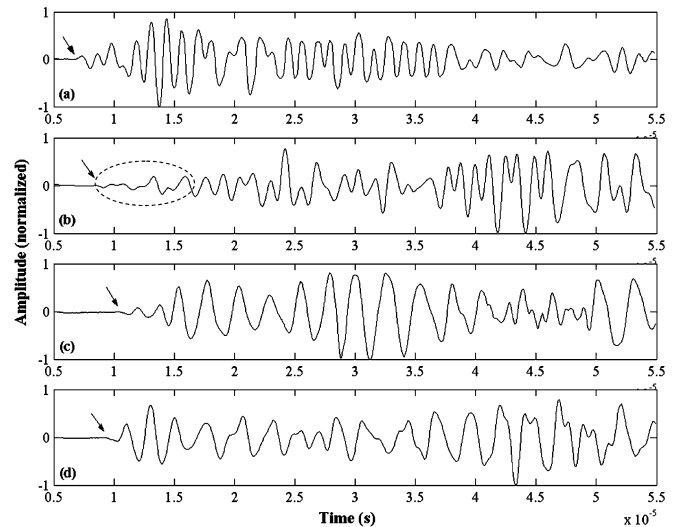


Fig. 6. Ultrasound signal waveforms from an animal taken: (a) from intact bone before osteotomy, (b) immediately after osteotomy, (c) at the seventh, and (d) at the fourteenth postoperative week. The arrows indicate the FAS that is used for the determination of the propagation velocity. The dotted circle depicts a low-amplitude wave representing a wave mode that is not present in later healing stages.

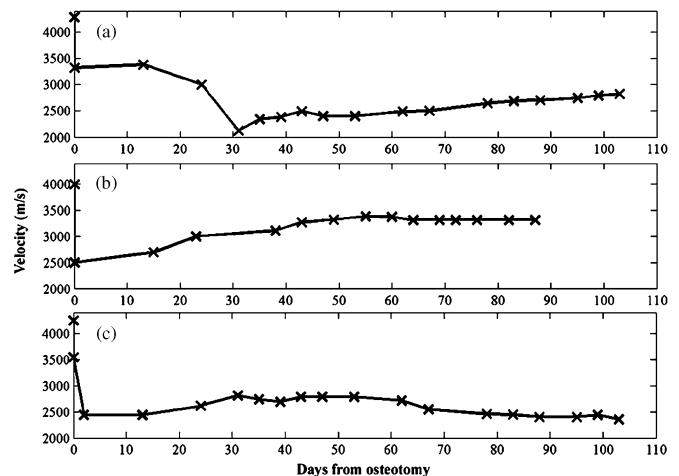


Fig. 7. Three velocity evolution patterns observed for three animals corresponding to: (a) secondary healing, (b) direct healing, and (c) delayed union.

osteotomy was reduced from the intact bone value by 715.6 (± 438.0) m/s. The velocity kept decreasing up to a turning-point, beyond which the velocity increased until the endpoint of the study. On average, the turning point took place on the 38.5 (± 6.4) day and the velocity reduction at this point was 730.3 (± 389.5) m/s compared to that immediately after the osteotomy. The characteristics of the pattern and their average values for the animals in the group are shown in Fig. 8.

Radiographic evidence demonstrated that secondary healing took place for the animals in the group, which is the most frequent healing type when an external fixation device is used. The decrease in velocity during the first postoperative weeks (the part between points B and C in Fig. 8) can be largely explained by the bone inflammatory response and the increased osteoclastic activity that occur at the early stages of secondary healing and cause bone resorption and further broadening of the

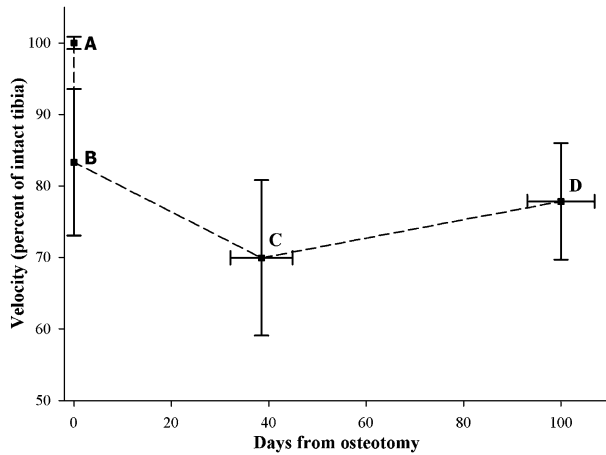


Fig. 8. The average pattern of velocity evolution over the healing period for 19 animals exhibiting secondary healing is presented. Point A refers to the velocity of intact bone, B to that of the osteotomized bone, C to the turning point beyond which velocity increases, and D to the velocity measured just before the endpoint of the study. The values in the y axis represent the average percentage of the intact bone velocity \pm one standard deviation. The error bar in the x axis at the point C represents the average days of the occurrence of the turning-point and its standard deviation, and the x axis error bar at D shows the mean and standard deviation of the last postoperative day.

fracture gap. The decrease might be additionally attributed to a different mode of propagation with a different wave velocity. As shown in Fig. 6(b), the FAS from the osteotomized bone is a low-amplitude wave corresponding to a different wave mode that was not present in the following signals. The average time for the attenuation of this wave mode was 28.1 ± 13.3 days, which is close to the timing of the turning point. Finally, as healing progresses, mineral and mechanical changes in callus resulted in a gradual velocity increase (part CD in Fig. 8). However, the transition of the velocity from B to C and from C to D was different for each animal.

In the second velocity pattern [Fig. 7(b)], velocity increased steadily after the osteotomy, revealing a different healing pathway. For this animal group, radiographic evaluation demonstrated that direct (primary) healing occurred. In this healing type, the fracture margins are not absorbed, but rather a direct bone union takes place across the fracture gap. Direct healing occurs in cases of rigid fixation combined with perfect bone fragments reduction (in our situation caused from the fine saw-produced osteotomy).

Fig. 7(c) illustrates an irregular evolution throughout the healing time. Despite an initial drop in velocity, no other systematic change in velocity was observed. Such peculiar velocity behavior was observed for two animals with no signs of radiographic healing.

Furthermore, the relation between radiographic healing and the velocity of ultrasound was examined. The animals were divided into two healing groups; the first includes radiographically healed bones and the second nonhealed bones. Assessment of radiographic healing was based on the three-bridged cortices criterion, as evaluated by observer A and B. Table I contains the average velocity, measured on the last postoperative day, and its percentage of the intact bone value (before osteotomy) for each healing group. On average, the velocity was higher for the healed bones, however, the difference between the

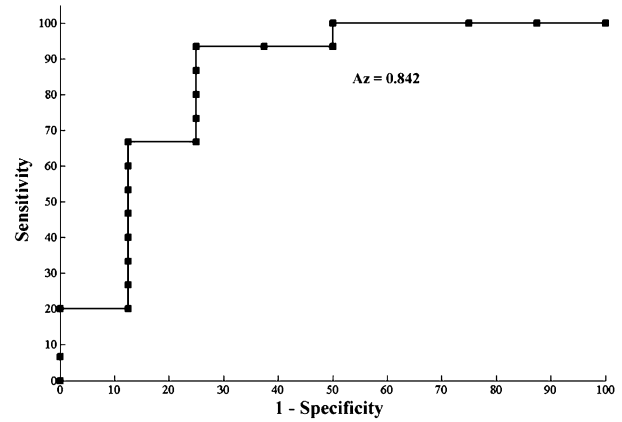


Fig. 9. ROC curve for the assessments made by observer A, when the criterion (threshold) was the velocity expressed as a percentage of the intact bone value. The area A_z under the curve was 0.842 (95% Confidence Interval = 0.630 to 0.958).

healing groups was statistically significant at $p < 0.05$ according to only observer A (p -value = 0.012 for the absolute and 0.008 for the percentage value, Wilcoxon nonparametric test). Moreover, the ability of the velocity, measured on the last postoperative day, to discriminate between radiographically healed and nonhealed animals was measured using the area A_z under a ROC curve. The ROC curve was generated by plotting the true positive fraction (sensitivity) against the false positive fraction (1-specificity) at different velocity values (criterion values). Fig. 9 illustrates the calculated ROC curve for the assessments made by observer A, when the velocity criterion was expressed as a percentage of the intact bone value. In that case A_z was 0.842 (95% Confidence Interval = 0.630 to 0.958). Table I also includes the densitometric and biomechanical data of each healing group, in absolute values and as a percentage of the contralateral bone. The stiffness, Young's modulus and ultimate strength were significantly higher for the healed bones, as assessed by observer B, whereas callus density and absolute values of Young's modulus and ultimate strength did not significantly differ between the groups that were assessed by observer A. The inter-observer agreement on the assessment of radiographic healing was found significant (p -value = 0.505, McNemar's test).

We also investigated whether the velocity measured on the last postoperative day has a significant correlation coefficient with the biomechanical and material properties of the healing bone. Fig. 10 illustrates the correlation of velocity with the square root of the Young's modulus (0.808, p -value < 0.001) and the average BMD (0.814, p -value < 0.001). Table II contains the correlation coefficient of ultrasound with the stiffness, Young's modulus and ultimate strength.

V. DISCUSSION

Medical wearable systems have found numerous clinical applications for the management of patients in home and outdoor environments. USBone constitutes the first such system in the field of orthopaedics for the long-term monitoring and therapy of bone fracture healing. The innovative elements of the system are the transducers' implantation adjacent to the fracture site,

TABLE I
ABSOLUTE AND PERCENTAGE VALUES OF VELOCITY (MEASURED ON THE LAST POSTOPERATIVE DAY), CALLUS BMD, STIFFNESS, YOUNG’S MODULUS, AND ULTIMATE STRENGTH OF RADIOGRAPHICALLY HEALED AND NON-HEALED BONES, AS ASSESSED BY OBSERVER A AND B

	Intact Tibia (n = 22)	Observer A			Observer B		
		Healed bone (n = 14)	Non-healed bone (n = 8)*	p-value	Healed bone (n = 13)	Non-healed bone (n = 9)*	p-value
Velocity (m/sec)	4275 (± 31.9)	3548 (± 344)	3066 (± 456)	0.012	3498 (± 351)	3196 (± 543)	0.147
Velocity percentage (healing / intact)	–	82.3% (± 8.1)	72.0% (± 10.3)	0.008	80.8% (± 7.9)	74.8% (± 12.9)	0.131
BMD (mg/cm ³)	1563 (± 81.6)	906 (± 218)	786 (± 121)	0.192	932 (± 218)	756 (± 71.8)	0.029
BMD percentage (callus / cortical from contralateral)	–	57.5% (± 16.2)	51.4% (± 10.1)	0.459	60.2% (± 16.2)	47.4% (± 4.5)	0.048
Stiffness (N/mm)	1714 (± 394)	1213 (± 463)	588 (± 203)	0.005	1291 (± 444)	623 (± 196)	0.003
Stiffness percentage (healing / contralateral)	–	68.9% (± 24.1)	38.6% (± 18.4)	0.005	73.7% (± 22.1)	38.4% (± 15.3)	0.004
Young’s Modulus (GPa)	13.89 (± 3.21)	4.72 (± 3.58)	1.66 (± 1.25)	0.089	5.21 (± 3.61)	1.67 (± 1.15)	0.020
Young’s Modulus percentage (healing / contralateral)	–	33.8% (± 26.6)	10.9% (± 6.1)	0.008	37.6% (± 26.6)	10.4% (± 5.8)	0.006
Ultimate Strength (MPa)	119.2 (± 22.5)	45.03 (± 30.0)	17.18 (± 11.4)	0.089	49.16 (± 29.9)	17.47 (± 10.6)	0.029
Ultimate Strength percentage (healing / contralateral)	–	38.5% (± 25.9)	14.3% (± 7.4)	0.008	42.5% (± 25.5)	13.8% (± 7.0)	0.003

*The 2 fracture cases with no sign of healing are not included in the non-healed bone group.

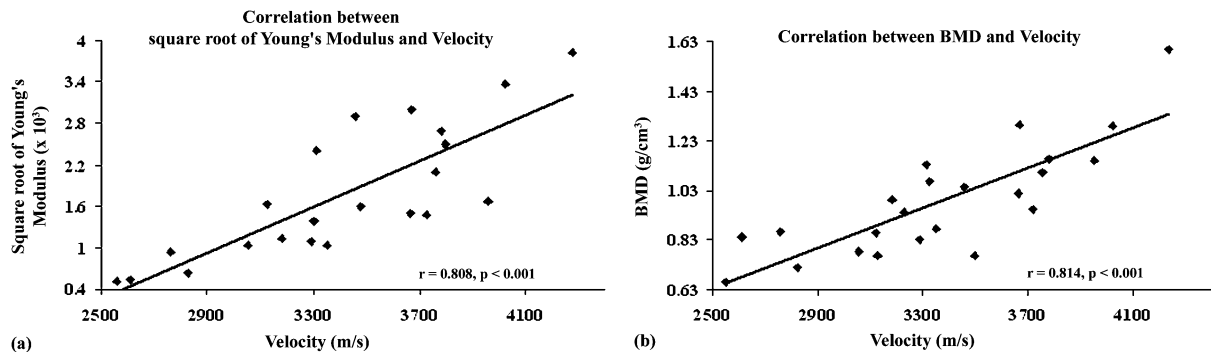


Fig. 10. The correlation of velocity, measured on the last postoperative day, with (a) the square root of Young’s Modulus and (b) the average BMD of callus.

TABLE II
CORRELATION COEFFICIENTS BETWEEN VELOCITY (MEASURED ON THE LAST POSTOPERATIVE DAY) AND BENDING STIFFNESS, YOUNG’S MODULUS, AND ULTIMATE STRENGTH

	Velocity	
	correlation coefficient (r)	p-value
Stiffness	0.699	0.004
Young’s Modulus	0.740	0.002
Ultimate Strength	0.754	0.001

a new wearable ultrasound device and a wireless platform that supports the communication between the patient and a centralized patient management system.

The performance of the USBone system was successfully tested and validated on a preclinical study. The preindustrial

prototype of the wearable device performed to expectation and the wireless transmission of the collected measurements was efficient and reliable. In order to address the clinical acceptance of our system, the wearable device has been divided into two light and small subsystems; the SM can be easily mounted on the frame of the external fixation and the CM can also be carried on the patient’s belt. Participating in the study orthopaedic surgeons found the centralized unit to meet the requirements of an integrated patient management system and to efficiently allow the remote monitoring of multiple patients.

The animal study was also used to evaluate the application of the ultrasound transducers. The performance of a midshaft transverse osteotomy offers a well-controlled and repeatable fracture model for the standardization of the implantation. The surgeons claim that the implantation of the transducers does not interfere with the surgical procedure neither increases the required time. The transducers are removed when the pins and

the frame of the external fixation device are also removed. No negative findings were observed from the use of implants. However, the transducers' placement involves an invasive procedure, as opposed to the transcutaneous ultrasound systems, fact that makes USBone applicable to open fractures treated with external fixation devices.

The animal experiment provided also with an ultrasound dataset necessary for the construction of the monitoring capabilities of the system. The dataset was developed from serial measurements taken on a 4-day basis, which are also annotated by follow-up radiographs, QCT-based densitometry and biomechanical data. Analysis of the radiographs was used as the Golden Standard for assessing bony union, although the process is largely dependent on orthopaedic surgeon's experience and skills [1], [40]. A systematic methodology was presented for 1) the segmentation of callus from the cortical bone and 2) the measurement of callus BMD from the 3-D image. Biomechanical data were derived from a three-point bending testing, which is a common modality for measuring the mechanical strength of cortical bone [3], [38]. The center of mass and the CSMI were computationally determined by the corresponding QCT slices, whereas the Young's modulus and ultimate strength were calculated from formulas developed for isotropic beams with uniform cross-section. It has been reported that the method error for long bones ranges from 7.3%–15.2% [3]. Although it is known that torsional testing is more suitable than bending when examining the properties of long bones, the authors were not able to perform torsional testing due to lack of equipment.

We showed that the velocity of radiographically healed bones, measured on the last postoperative day, exceeds on average 80% that of the intact bone value. This finding is consistent with similar animal [14] and clinical studies [15], [17], [20]. On the other hand, the material and mechanical properties of healed bones reached lower percentage values of those of contralateral intact bones (range from 33.8 to 68.9%). ROC analysis was performed to investigate the ability of ultrasound to discriminate between healed and nonhealed bones. The highest discriminate power was found for the clinical assessments of observer A ($A_z = 0.842$), when ultrasound velocity is expressed as a percentage of the intact bone value. The capability of ultrasound to represent the mechanical and material properties of the healing bone was also demonstrated. The correlation coefficient of velocity with the callus BMD, stiffness, ultimate strength, absolute and square root of Young's modulus is characterized as good-to-perfect and is higher than similar studies [16], [20]. The authors attribute the higher correlation values to the increased repeatability and accuracy of the transosseous measurements.

It was also demonstrated that the pattern of velocity evolution monitors a dynamic healing process. The initial decrease in velocity, for the secondary healing type, is consistent with the findings of previous clinical studies [15], [17]. Gerlanc *et al.* [15] reports that a 24% decrease from the contralateral bone value is observed within a few days of fracture. This is followed by an additional 7% decrease until the end of the first month, which is caused from the metabolic and structural changes of bone. Our results indicated an average 17% drop (point B in Fig. 8) after osteotomy and a further 13% up to the 38.5 day (point C in

Fig. 8). Theoretically, the velocity through a bone (of 4275 m/s nominal velocity) with a 2-mm gap and a 25-mm distance between the transducers decreases by 17.1%. Also, in our study the existence of the turning point is explained on the grounds of the secondary healing biology and of a change in the wave mode of FAS. This mode corresponds to a low-amplitude lateral wave propagating across the newly formatted callus; as healing progresses, the mode is highly attenuated. Further investigation is, however, needed in order to draw clear conclusions about the nature of this propagation mode

Nevertheless, the propagation velocity of the FAS is only an apparent value and mainly gives information about the bone subsurface. A large number of additional waveform features can be extracted from the received signals. However, our previous study on features, such as signal duration, energy, amplitude of the first extrema and central frequency, has not shown any specific variation pattern over the healing period [25]. We believe that features lying both in the time and frequency domain can capture the various wave phenomena [41] associated with the propagation of ultrasound within the bounded dimensions of bone. Computational [22]–[25] and experimental [19], [22], [24], [26] studies have shown that the received signal is a superposition of numerous wave modes, each one exhibiting velocity dispersion, attenuation, and other characteristics. However, no work has been focused on the investigation of guided waves through healing bones.

Our current research also involves the evaluation of the system on human fracture cases. The clinical application of USBone is associated with significant clinical, social and economical factors. Amongst the clinical benefits is the provision to the health professionals of a monitoring system to assist in the decision-making process. In addition, the doctors can remotely follow multiple patients and prescribe individualized monitoring and therapy plans according to the patient needs. Furthermore, the novel use of implants does not restrict the application of the system to only peripheral skeletal sites, such as the tibia and radius. The main potential social and economical impact of our system is that the wireless platform of the system may reduce the follow-up visits of the patient to the orthopaedist's office and makes possible the management of patients in out-hospital environments and geographically remote areas. The wearable device supports the remote collection of measurements and the automated application of LiUS for a prolonged period of time. In this sense, the system supports patient comfort and welfare and ensures early return to everyday activities.

Our future work will focus on the exploitation of the ultrasonic features for the construction of a decision-making mechanism into the system.

VI. CONCLUSION

We presented a telemedicine system for the ultrasonic monitoring and acceleration of bone fracture healing. The novelty of the system consists in that the transducers are implanted adjacent to the fracture site allowing for transosseous wave propagation and the wearable platform supports the wireless communication of data from the patient's site to a centralized

unit. The system was tested and validated on an animal study demonstrating its ability to collect and wirelessly transmit ultrasound measurements in an effective and reliable way. Furthermore, participating in the study orthopaedic surgeons initially accepted the system for clinical application. Analysis of the acquired measurements indicated that the velocity of propagation is a significant feature which describes a dynamic healing process and correlates with the radiographic, material and mechanical properties of the bone. Incorporation of a decision-making mechanism into the system may address the need for the quantitative and objective assessment of fracture healing. However, the conclusions drawn from the preclinical system application cannot be extrapolated to the evaluation of human fractures. We will present results from clinical trials in the near future.

ACKNOWLEDGMENT

The authors are grateful to ANCO S.A., Greece, for the implementation of the USBone device in the framework of the USBone project.

REFERENCES

- [1] T. J. Blokhuis, J. H. D. de Bruine, J. A. M. Bramer, F. C. den Boer, F. C. Bakker, P. Patka, H. J. T. M. Haarman, and R. A. Manoliu, "The reliability of plain radiography in experimental fracture healing," *Skeletal Radiol.*, vol. 30, pp. 151–156, 2001.
- [2] P. Augat, J. Merk, H. K. Genant, and L. Claes, "Quantitative assessment of experimental fracture repair by peripheral computed tomography," *Calcif. Tissue Int.*, vol. 60, pp. 194–199, 1997.
- [3] T. Jamsa, P. Jalovaara, Z. Peng, H. K. Vaananen, and J. Tuukkanen, "Comparison of three-point bending test and peripheral quantitative computed tomography analysis in the evaluation of the strength of mouse femur and tibia," *Bone*, vol. 23, no. 2, pp. 155–161, 1998.
- [4] F. C. den Boer, J. A. Bramer, P. Patka, F. C. Bakker, R. H. Barentsen, A. J. Feilzer, E. S. de Lange, and H. J. Haarman, "Quantification of fracture healing with three-dimensional computed tomography," *Arch Orthop Trauma Surg*, vol. 117, pp. 345–350, 1998.
- [5] J. B. Richardson, J. L. Cunningham, A. E. Goodship, B. T. O'Connor, and J. Kenwright, "Measuring stiffness can define healing of tibial fractures," *J. Bone Joint Surg Br.*, vol. 76, pp. 389–394, 1994.
- [6] K. M. Shah, A. C. Nicol, and D. L. Hamblen, "Fracture stiffness measurement in tibial shaft fractures: A noninvasive method," *Clin. Biomech.*, vol. 10, no. 8, pp. 395–400, 1995.
- [7] R. Hente, J. Cordey, and S. M. Perren. (2003, Mar.) *In vivo* measurement of bending stiffness in fracture healing. *Biomed. Eng. Online* [Online], vol (3). Available: <http://www.biomedical-engineering-online.com/content/2/1/8>
- [8] L. D. Nokes and G. C. Thorne, "Vibrational analysis in the assessment of conservatively managed tibial fractures," *J. Biomed. Eng.*, vol. 7, pp. 40–44, 1985.
- [9] G. Van der Perre and G. Lowet, "In vivo assessment of bone mechanical properties by vibration and ultrasonic wave propagation analysis," *Bone*, vol. 18, no. 1, pp. 29S–35S, Jan. 1996.
- [10] Y. Nakatsuchi, A. Tsuchikane, and A. Nomura, "The vibrational mode of the tibia and assessment of bone union in experimental fracture healing using the impulse response method," *Med. Eng. Phys.*, vol. 18, no. 7, pp. 575–583, 1996.
- [11] Y. Hirasawa, S. Takai, W. Kim, N. Takenaka, N. Yoshino, and Y. Wantabe, "Biomechanical monitoring of healing bone based on acoustic emission technology," *Clin Orthop.*, no. 402, pp. 236–244, 2002.
- [12] N. Maffuli and A. Thornton, "Ultrasonographic appearance of external callus in long-bone fractures," *Injury*, vol. 26, no. 1, pp. 5–12, 1995.
- [13] T. Anast, T. Fields, and A. Hiseth, "Ultrasonic technique for the evaluation of bone fracture," *Am. J. Phys Med.*, vol. 37, pp. 157–157, 1958.
- [14] W. Abendschein and G. W. Hayatt, "Ultrasonics and physical properties of healing bone," *J. Trauma*, vol. 12, pp. 297–301, 1972.
- [15] M. Gerlanc, D. Haddad, G. W. Hyatt, J. T. Langloh, and P. S. Hillaire, "Ultrasonic study of normal and fractured bone," *Clin. Orth. Rel. Res.*, vol. 111, pp. 175–180, 1975.
- [16] P. J. Gill, G. Kernohan, I. N. Mawhinney, R. A. Mollan, and R. McIlhagger, "Investigation of the mechanical properties of bone using ultrasound," *Proc. Inst. Mech. Eng. [H]*, vol. 203, no. 1, pp. 61–63, 1989.
- [17] J. L. Cunningham, J. Kenwright, and C. J. Kershaw, "Biomechanical measurement of fracture healing," *J. Med. Eng. Tech.*, vol. 13, no. 3, pp. 92–101, 1990.
- [18] J. Saulgozis, L. Pontaga, and G. Van Der Perre, "The effect of fracture and fracture fixation on ultrasonic velocity and attenuation," *Physiol. Meas.*, vol. 17, no. 3, pp. 201–211, 1996.
- [19] G. Lowet and G. Van der Perre, "Ultrasound velocity measurements in long bones: Measurement method and simulation of ultrasound wave propagation," *J. Biomech.*, vol. 29, no. 10, pp. 1255–1262, 1996.
- [20] E. Maylia and L. D. Nokes, "The use of ultrasonics in orthopaedics—A review," *Technol. Health Care*, vol. 7, pp. 1–28, 1999.
- [21] V. C. Protopappas, D. Baga, D. I. Fotiadis, A. Likas, A. Papachristos, and K. N. Malizos, "An intelligent wearable system for the monitoring of fracture healing of long bones," in *Proc EMBC'02, IFMBE, 2002*, pp. 978–979.
- [22] E. Camus, M. Talmant, G. Berger, and P. Laugier, "Analysis of the axial transmission technique for the assessment of skeletal status," *J. Acoust. Soc. Am.*, vol. 108, no. 6, pp. 3058–3065, Dec. 2000.
- [23] E. Bossy, M. Talmant, and P. Laugier, "Effect of cortical thickness on velocity measurements using ultrasonic axial transmission: A 2-D simulation study," *J. Acoust. Soc. Am.*, vol. 112, no. 1, pp. 297–307, Jul. 2002.
- [24] P. H. F. Nicholson, P. Moilanen, T. Karkkainen, J. Timonen, and S. Cheng, "Guided ultrasonic waves in long bones: Modeling, experiment and *in vivo* application," *Phys. Meas.*, vol. 23, pp. 755–768, 2002.
- [25] V. C. Protopappas, I. C. Kourtis, D. I. Fotiadis, and C. V. Massalas, "Finite element modeling of ultrasound propagation in fractured long bones," in *Proc. IASTED Int. Conf. Biomechanics*, 2003, pp. 54–58.
- [26] C. Njeh, D. Hans, C. Wu, E. Kantorovich, M. Sister, T. Fuerst, and H. Genant, "An *in vitro* investigation of the dependence on sample thickness of the speed of sound along the specimen," *Med. Eng. Phys.*, vol. 21, pp. 651–659, 1999.
- [27] L. R. Duarte, "The stimulation of bone growth by ultrasound," *Arch. Orthop. Trauma Surg.*, vol. 101, pp. 153–159, 1983.
- [28] J. D. Heckman, J. P. Ryaby, J. McCabe, J. J. Frey, and R. F. Kilcoyne, "Acceleration of tibial fracture-healing by noninvasive, low-intensity pulsed ultrasound," *J. Bone Joint Surg. Am.*, vol. 76, no. 1, pp. 26–34, Jan. 1994.
- [29] T. K. Kristiansen, J. P. Ryaby, J. McCabe, J. J. Frey, and L. R. Roe, "Accelerated healing of distal fractures with the use of specific, low-intensity ultrasound. A multicenter, prospective, randomized, double-blind, placebo-controlled study," *J. Bone Joint Surg. Am.*, vol. 79, no. 7, pp. 961–973, Jul. 1997.
- [30] C. Rubin, M. Bolander, J. P. Ryaby, and M. Hadjiargyrou, "The use of low-intensity ultrasound to accelerate the healing of fractures," *J. Bone Joint Surg. Am.*, vol. 83, no. 2, pp. 259–270, Feb. 2001.
- [31] E. Mayr, V. H. Frankel, and A. Ruter, "Ultrasound—An alternative healing method for nonunions?," *Arch. Orthop. Trauma Surg.*, vol. 120, pp. 1–8, 2000.
- [32] M. E. Hantes, A. N. Mavrodontidis, C. G. Zalavras, A. H. Karantanas, T. Karachalios, and K. N. Malizos, "Low-Intensity transosseous ultrasound accelerates osteotomy healing in a sheep fracture model," *J. Bone Joint Surg. Am.*, vol. 86, no. 10, pp. 2275–2282, Oct. 2004.
- [33] J. D. Heckman and J. Sarasohn-Kahn, "The economics of treating tibia fractures. The cost of delayed unions," *Bull. Hosp. Joint. Dis.*, vol. 56, pp. 63–72, 1997.
- [34] P. Bonato, "Wearable sensors/systems and their impact on biomedical engineering," *IEEE Eng. Med. Biol. Mag.*, vol. 22, no. 3, pp. 18–20, May/Jun. 2003.
- [35] M. J. Tierney, J. A. Tamada, R. O. Potts, L. Jovanovic, and S. Garg, "Clinical evaluation of the glucoWatch® biographer: A continual, noninvasive glucose monitor for patients with diabetes," *Biosens. Bioelectron.*, vol. 16, pp. 621–629, 2001.
- [36] K. Van Laerhoven, A. Schmidt, and H. W. Gellersen, "Multi-sensor context aware clothing," in *Proc. 6th Int. Symp. Wear. Comp.*, 2002, pp. 49–56.
- [37] Food and Drug Administration, Washington, DC, "Biological Evaluation of Medical Devices," FDA-Modified ISO-10993, pt. Part 1, 1995.
- [38] C. H. Turner and D. B. Burr, "Basic biomechanical measurements of bone: A tutorial," *Bone*, vol. 14, pp. 595–608, 1993.
- [39] S. C. Cowin, *Bone Mechanics*. Boca Raton, FL: CRC Press, 1991.

- [40] D. B. Whelan, M. Bhandari, M. D. McKee, G. H. Guyatt, H. J. Kreder, D. Stephen, and E. H. Schemitsch, "Interobserver and intraobserver variation in the assessment of the healing of tibial fractures after intramedullary fixation," *J. Bone. Joint. Surg. Br.*, vol. 84, no. 1, pp. 15–18, 2002.
- [41] J. L. Rose, *Ultrasonic Waves in Solid Media*. Cambridge, U.K.: Cambridge University Press, 1999.



Vasilios C. Protopappas (S'04) was born in Ioannina, Greece, in 1976. He received the Diploma degree in electrical and computer engineering from the National Technical University of Athens, Athens, Greece, in 1999 and the M.Sc. in Bioengineering from the University of Strathclyde, Glasgow, U.K., in 2000. He is currently working toward the Ph.D. degree at the Department of Medical Physics, Medical School, University of Ioannina.

Since 2000, he has been with the Unit of Medical Technology and Intelligent Information Systems, University of Ioannina. His research interests include biomechanics, ultrasonic testing and finite element modeling.



Dina A. Baga was born in Ioannina, Greece, in 1976. She received the B.Sc. degree in computer science from the University of Ioannina in 1997.

Since 1997, she has been with the Unit of Medical Technology and Intelligent Information Systems, University of Ioannina, where she is the Head of the Software Engineering Team. Her research interests include biomedical technology, intelligent information systems, and wearable systems in healthcare.



Dimitrios I. Fotiadis (M'01) was born in Ioannina, Greece, in 1961. He received the Diploma degree in chemical engineering from the National Technical University of Athens, Athens, Greece, and the Ph.D. degree in chemical engineering from the University of Minnesota, Minneapolis, in 1990.

Since 1995, he has been with the Department of Computer Science, University of Ioannina, Greece, where he is currently an Associate Professor. He is the director of the Unit of Medical Technology and Intelligent Information Systems. His research interests include biomedical technology, biomechanics, scientific computing and intelligent information systems.



Aristid C. Likas (S'91–M'96–SM'03) was born in Athens, Greece, in 1968. He received the Diploma degree in electrical engineering and the Ph.D. degree in electrical and computer engineering both from the National Technical University of Athens, Athens, Greece.

Since 1996, he has been with the Department of Computer Science, University of Ioannina, Ioannina, Greece, where he is currently an Assistant Professor. His research interests include neural networks, machine learning, pattern recognition, and intelligent systems for biomedical engineering.



Athanasios A. Papachristos was born in Lamia, Greece, in 1965. He received the Diploma degree in medicine from the Faculty of Medicine, the Aristotle University of Thessaloniki, Thessaloniki, Greece, in 1992. Since 2000, he is working toward the Ph.D. degree at the Department of Medicine, School of Health Sciences, University of Thessalia, Larissa, Greece.

He has trained in Orthopaedics at the University Hospital of Larissa, Greece. Currently, he is doing a clinical fellowship at St. Josef Hospital, Department of Shoulder and Elbow Surgery, Essen Kupferdreh, Germany. His research interests include biomechanics and fracture healing enhancement.



Konstantinos N. Malizos was born in Larissa, Greece, in 1954. He received the Diploma degree in Medicine from the Faculty of Medicine, the Aristotle University of Thessaloniki, Thessaloniki, Greece, in 1978 and the Ph.D. degree from the Medical School, University of Ioannina, Ioannina, Greece, in 1986.

He has trained in Orthopaedics at the University Hospital of Ioannina, Greece, "SOS-MAIN" Strasbourg, France, in 1988, Duke University Medical Center, Durham, NC, from 1988 to 1991. Since 1997, he is a Professor and Chairman of Orthopaedics at the School of Health Sciences, University of Thessalia, Larissa. He has published 71 international and 24 national papers in peer review journals, 10 book chapters and one book as editor-author.

Prof. Malizos is a member of ten scientific societies, Vice President of the European Bone and Joint Infection Society (2003–2005), and President elect (2005–2007). He has received eight international awards and prizes.